The American Journal of Pathology, Vol. 184, No. 12, December 2014

ELSEVIER

The American Journal of PATHOLOGY

ajp.amjpathol.org

SHORT COMMUNICATION

Blood Vascular Abnormalities in *Rasa1*^{R780Q} Knockin Mice

Implications for the Pathogenesis of Capillary Malformation—Arteriovenous Malformation

Beth A. Lubeck,* Philip E. Lapinski,* Timothy J. Bauler,* Jennifer A. Oliver,* Elizabeth D. Hughes,† Thomas L. Saunders,†‡ and Philip D. King*

From the Department of Microbiology and Immunology, the Biomedical Research Core Facility Transgenic Animal Model Core† and the Division of Molecular Medicine and Genetics,‡ Department of Internal Medicine, University of Michigan Medical School, Ann Arbor, Michigan*

Accepted for publication August 14, 2014.

Address correspondence to Philip D. King, Ph.D., Department of Microbiology and Immunology, University of Michigan Medical School, 6606 Med Sci II, 1150 W Medical Center Dr, Ann Arbor, MI 48109-5620. E-mail: kingp@umich.edu.

Capillary malformation—arteriovenous malformation (CM-AVM) is an autosomal dominant blood vascular (BV) disorder characterized by CM and fast flow BV lesions. Inactivating mutations of the *RASA1* gene are the cause of CM-AVM in most cases. RASA1 is a GTPase-activating protein that acts as a negative regulator of the Ras small GTP-binding protein. In addition, RASA1 performs Ras-independent functions in intracellular signal transduction. Whether CM-AVM results from loss of an ability of RASA1 to regulate Ras or loss of a Ras-independent function of RASA1 is unknown. To address this, we generated *Rasa1* knockin mice with an R780Q point mutation that abrogates RASA1 catalytic activity specifically. Homozygous *Rasa1*$^{R780Q/R780Q}$ mice showed the same severe BV abnormalities as *Rasa1*-null mice and died midgestation. This finding indicates that BV abnormalities in CM-AVM develop as a result of loss of an ability of RASA1 to control Ras activation and not loss of a Ras-independent function of this molecule. More important, findings indicate that inhibition of Ras signaling is likely to represent an effective means of therapy for this disease. *(Am J Pathol 2014, 184: 3163—3169; http://dx.doi.org/10.1016/j.ajpath.2014.08.018)*

Capillary malformation—arteriovenous malformation (CM-AVM) is an autosomal dominant blood vascular (BV) disorder that affects at least 1:100,000 individuals in Northern European populations.[1–3] The pathognomonic feature of CM-AVM is the presence of one or more randomly distributed cutaneous CMs. In one third of patients, there are additional fast flow lesions that include AVM, arteriovenous fistulas, and Parkes-Weber syndrome. Complications of CM-AVM include hemorrhage, epilepsy, hydrocephalus, cardiac failure, and death. Inactivating mutations of the *RASA1* gene, which encodes the p120 Ras GTPase-activating protein (p120 Ras-GAP or RASA1), are the cause of CM-AVM in most patients. Mutations are distributed throughout the length of the gene, and most are nonsense mutations, insertions, and deletions resulting in frameshifts or disruption of splice sites.[1–9] Although not proved, it is likely that all of these mutations result in complete null alleles because transcripts would be rapidly degraded by nonsense-mediated RNA decay.[10] Only one germline *RASA1* allele is affected in CM-AVM, and it has been postulated that somatic second hit inactivating mutations in the inherited normal *RASA1* allele are required for lesion development.[2]

As a Ras-GAP, one recognized function of RASA1 is to inactivate the Ras small GTP-binding protein.[11] Ras is an intracellular membrane-tethered signaling protein that is converted from an inactive GDP-bound to an active GTP-bound state in response to growth factor stimulation.[12] In its active state, Ras stimulates several different downstream enzymatic cascades that include the mitogen-activated protein kinase (MAPK) cascade and the phosphatidylinositol 3-kinase

Supported by NIH grant RO1 HL096498 (P.D.K.) and American Heart Association grants 12PRE8850000 and 11POST7580023 (B.A.L. and P.E.L., respectively). The Transgenic Mouse Core was supported in part by the NIH through the University of Michigan's Cancer Center support grant P30 CA046592.

Disclosures: None declared.

http://dx.doi.org/10.1016/j.ajpath.2014.08.018

(PI3K) signaling pathway that drive cell growth, proliferation, differentiation, and survival.[13–15] Ras-GAPs inactivate Ras by inserting an arginine finger, located in a GAP domain, into the Ras catalytic site, thereby increasing the ability of Ras to hydrolyze bound GTP to GDP by several orders of magnitude.[16] However, RASA1 is also able to participate in growth factor receptor signal transduction independent of an ability to inactivate Ras.[11]

Consistent with the BV lesions in patients with CM-AVM, mice that are homozygous for a null allele of *Rasa1* die by embryonic day 10.5 (E10.5) of gestation as a result of abnormal BV development.[17] At E9.5, endothelial cells (ECs) in the yolk sac are seen to assemble into a honeycombed pattern but then fail to reorganize into a vascular network that supplies blood to the embryo. In the embryo proper at E9.5, a narrow and irregular dorsal aorta is observed with abnormal projecting arteries. Local rupture of blood vessels and a distended pericardial sac are also apparent. The same phenotype is observed in conditional RASA1-deficient mice in which disruption of the *Rasa1* gene is restricted to ECs.[18]

It is unknown if dysregulated activation of the Ras pathway or loss of a Ras-independent function of RASA1 in ECs is responsible for the development of BV abnormalities in RASA1-deficient mice and humans. Therefore, to address this question, in the current studies, we generated a $Rasa1^{R780Q}$ knockin mouse that expresses a form of RASA1 that lacks an arginine finger. Previous studies have established that the R780Q mutation abrogates an ability of RASA1 to promote Ras hydrolysis of GTP.[19] BV development in homozygous $Rasa1^{R780Q}$ mice was assessed.

Materials and Methods

Gene Targeting

A $Rasa1^{R780Q}$ targeting construct was assembled in *p-loxP-2FRT-PGKneo*.[20] A 5′ arm that spanned introns 13 through 17 of the *Rasa1* gene was generated by PCR from a C57BL/6 genomic *Rasa1* BAC clone and inserted into the EcoRI/KpnI sites of the vector. The primers used were as follows: 5′ arm forward, 5′-GCGCGAATTCGCGGCCGCTTAGTCTTTC-AGGCATTTTATAGC-3′; and 5′ arm reverse, 5′-GCG-CGGTACCGAATGCTTATTTACCAGGAGTGAC-3′. A middle segment spanning intron 17 through 18 was generated by PCR from the same *Rasa1* BAC clone that contained an R780Q mutation in exon 18 that was generated by homologous recombination in *Escherichia coli* (CGA to CAA codon change). The middle fragment was inserted into the KpnI and 3′ BglII sites of the vector. The primers used were as follows: M forward, 5′-GCGC-GGTACCAGATCTAAATATTTGAGCCTATGAGGACC-ATTC-3′; and M reverse, 5′-GCGCGGATCCCATATCCA-ACTTCACATGATGTGC-3′. A 3′ arm that spanned introns 18 through 20 was generated by PCR from the wild-type *Rasa1* BAC clone and was inserted into the XhoI site of the vector. The primers used were as follows: 3′ arm forward, 5′-GCGCCTCGAGGAATTTCCCACATGGA-3′; and 3′ arm reverse, 5′-GCGCCTCGAGATATGTTGTCATGTAA-3′. The targeting construct was sequenced to verify the absence of any PCR-induced errors. The construct was electroporated into W4 embryonic stem (ES) cells that were subsequently cultured in neomycin. Genomic DNA from neomycin-resistant ES cell clones was analyzed by quantitative real-time PCR using an integration primer/probe set in which the 5′ and 3′ primers flanked the *FRT-NeoR-FRT* insertion site and the probe was complimentary to regions both 5′ and 3′ to the point of insertion.[21] Fold differences in the amount of exon 18 target relative to that in genomic DNA prepared from wild-type W4 ES cells were calculated as described.[22,23] Clones that demonstrated a twofold reduction in the intron 18 target were analyzed further by quantitative real-time PCR using a copy number primer/probe set based within exon 14 of the *Rasa1* gene (Life Technologies, Carlsbad, CA). Of those clones that contained diploid amounts of the exon 14 target, a long-range PCR was performed using a *Rasa1* forward primer based on the 5′ of the 5′ end of the *Rasa1* targeting vector insert and a reverse primer based in intron 18. A similar long-range PCR was performed using a forward primer based in intron 18 and a reverse primer located 3′ of the 3′ end of the *Rasa1* targeting vector insert. Both PCR products were sequenced to confirm the presence of the R780Q mutation within the endogenous *Rasa1* locus.

Two of several correctly targeted $Rasa1^{R780Q}$ clones were injected into C57BL/6J X (C57BL/6J X DBA/2) blastocysts to generate chimeric mice that were then bred with C57BL/6 actin promoter-driven *Flp* transgenic mice to achieve germline transmission of the targeted $Rasa1^{R780Q}$ allele and deletion of the *NeoR* cassette in intron 18.[24] Germline transmission and *NeoR* deletion were determined by PCR of tail genomic DNA prepared from agouti coat-colored progeny using a forward primer based in exon 18 and a reverse primer based 3′ to the 3′ *FRT* site in intron 18. Germline transmitted mice were then crossed with C57BL/6 mice and the same PCR was performed on tail DNA of progeny that had not inherited the *actin-Flp* transgene, also determined by PCR. This step was undertaken to obtain mice with confirmed germline deletion of the *NeoR* cassette within the $Rasa1^{R780Q}$ locus.

Embryonic Lethality

$Rasa1^{R780Q/+}$ mice were crossed with $Rasa1^{fl/fl}$ mice with an inserted *loxP* sequence in intron 18.[25] $Rasa1^{R780Q/fl}$ progeny were identified by PCR of tail genomic DNA using the same primers used above to detect deletion of the *NeoR* cassette. The expected PCR product sizes from the $Rasa1^{fl}$ and $Rasa1^{R780Q}$ alleles are 685 and 604 bp, respectively. $Rasa1^{R780Q/fl}$ mice were intercrossed, and *Rasa1* genotypes of embryonic and 3-week-old pups were determined by PCR of yolk sac and tail genomic DNA, respectively, as

described above. A χ^2 test was used to determine the probability that the frequency of observed genotypes of pups and embryos were consistent with a mendelian pattern of inheritance. Embryo images were acquired on an Olympus SZ61 dissecting microscope equipped with a digital camera (Lumenera, Ottawa, ON). All experiments performed on mice were in compliance with the University of Michigan (Ann Arbor, MI) guidelines and were approved by the University Committee on the Use and Care of Animals.

Western Blot Analysis

Individual E9.5 embryos were minced and digested in trypsin/EDTA (Life Technologies) at 37°C for 15 minutes. Murine embryonic fibroblasts (MEFs) were generated by culture of released cells in fibroblast media (Dulbecco's modified Eagle's medium, 10% fetal bovine serum, 1% penicillin/streptomycin, and 1% L-glutamine). At confluence, MEFs were harvested and 3×10^6 cells were lysed in 1% NP-40 lysis buffer. RASA1 protein abundance was determined by using Western blot analysis of cell lysates using an anti-RASA1 antibody (B4F8; Santa Cruz, Dallas, TX). Blots were stripped and reprobed with an anti–glyceraldehyde-3-phosphate dehydrogenase antibody (Santa Cruz) to ascertain equivalent protein loading.

Whole Mount Staining

E9.5 embryos were fixed in 1% paraformaldehyde in phosphate-buffered saline. Fixed embryos were stained with a rat anti-CD31 antibody (BD Biosciences, San Jose, CA), followed by a secondary goat anti-rat Ig Alexa Fluor 488 antibody (Invitrogen, Carlsbad, CA). Images of embryos were acquired on an Olympus BX60 upright fluorescence microscope equipped with a digital camera (Nikon, Tokyo, Japan).

Immunohistological Data

E9.5 embryos were fixed in formalin and embedded in paraffin. Sections (5 μm thick) were stained with a rabbit anti–phospho-extracellular signal regulated kinase (ERK) antibody (D13.14.4E; Cell Signaling, Danvers, MA), followed by biotinylated anti-rabbit Ig (Jackson Immunoresearch, West Grove, PA) and streptavidin–horseradish peroxidase with tyramide signal amplification (Perkin Elmer, Waltham, MA). Sections were then stained with a rat anti-CD31 antibody (sz31; Dianova, Hamburg, Germany), followed by secondary goat anti-rat Alexa Fluor 594 (Invitrogen). Some sections were stained with CD31 and secondary antibody alone or with hematoxylin and eosin. Images of sections were acquired as described in *Whole Mount Staining*.

Results

Embryonic Lethality of Homozygous *Rasa1*^{R780Q} Mice

A murine *Rasa1*^{R780Q} allele with an inserted *NeoR* cassette in intron 18 was generated by homologous recombination in ES cells (Figure 1). Of several correctly targeted euploid ES clones, two were injected into blastocysts. Chimeric mice derived from both clones were bred with transgenic mice that express the Flp recombinase under control of the actin promoter to achieve simultaneous germline transmission of

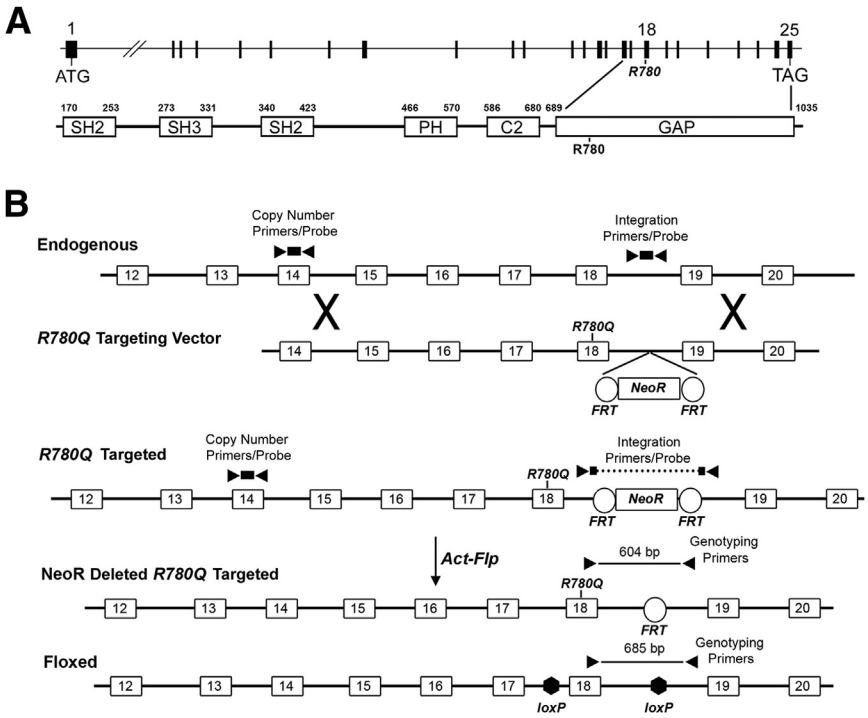

Figure 1 Generation of *Rasa1*^{R780Q} knockin allele in mice. **A:** Exon-intron organization of the murine *Rasa1* gene (top) and RASA1 protein (bottom). The positions of the R780Q and R780Q mutations in exon 18 and the GAP domain, respectively, are indicated. **B:** An R780Q targeting vector with an R780Q mutation in exon 18 and a *FRT*-flanked *NeoR* cassette in intron 18 is shown below the endogenous allele. At middle is shown the R780Q targeted allele before and after excision of the *NeoR* cassette achieved with an actin promoter-driven *Flp* transgene (*Act-Flp*). At bottom is depicted a *Rasa1* floxed allele in which exon 18 is flanked by *loxP* sites. Positions of real-time PCR primer/probe pairs used in the detection of ES cell homologous recombinants and PCR primer pairs used in mouse genotyping are indicated. C2, protein kinase C2 homology; GAP, GTPase-activating protein domain; PH, pleckstrin homology; SH2, Src homology 2; SH3, Src homology 3.

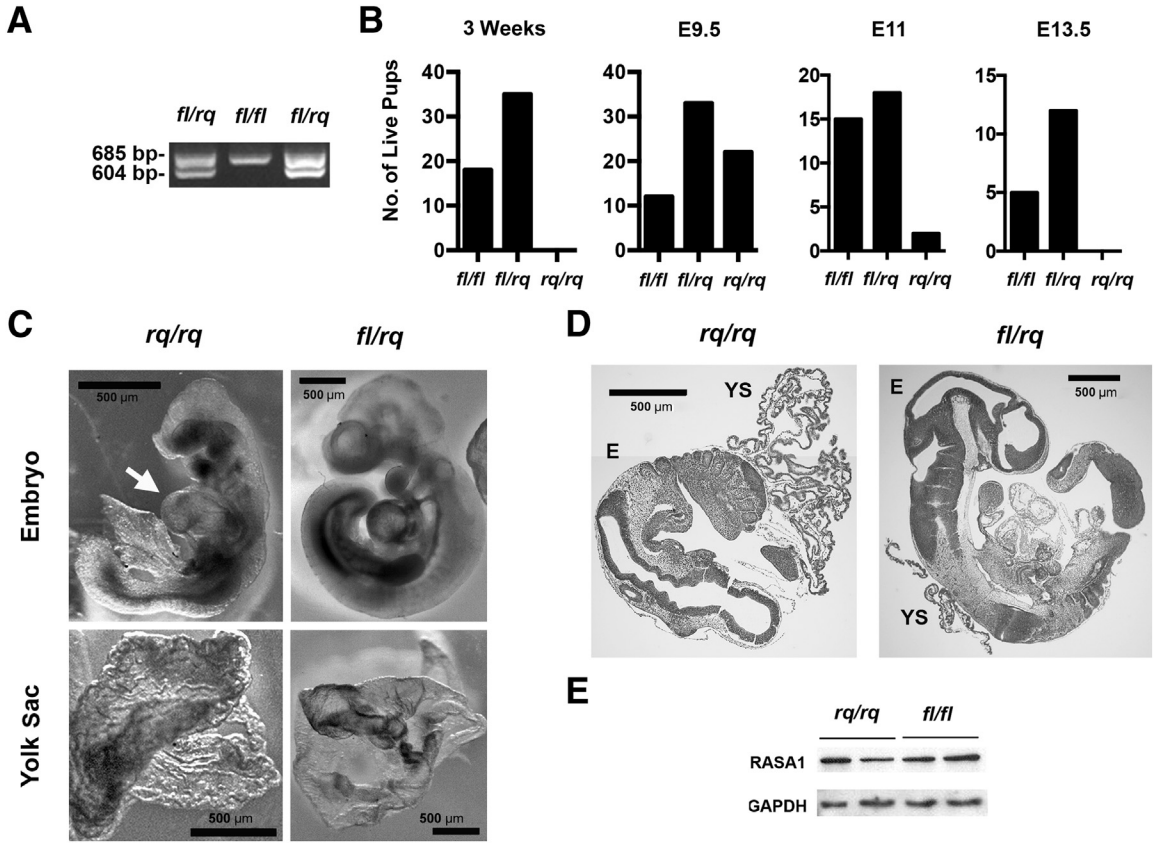

Figure 2 Embryonic lethality of homozygous *Rasa1*^{R780Q} mice. **A:** *Rasa1*$^{R780Q/fl}$ mice were intercrossed. Tail genomic DNA from progeny at 3 weeks of age was PCR amplified using genotyping primers indicated in Figure 1. Genotyping results from two *Rasa1*$^{R780Q/fl}$ (*fl/rq*) pups and one *Rasa1*$^{fl/fl}$ (*fl/fl*) pup are depicted. **B:** Graphs show the total number of pups of the indicated genotypes derived from intercrosses of *Rasa1*$^{R780Q/fl}$ mice determined at 3 weeks after birth and at E9.5, E11, and E13.5 of development. At E9.5, genotype frequencies are consistent with mendelian inheritance (χ^2 test). At E11, E13.5, and 3 weeks of age, genotype frequencies are not consistent with mendelian inheritance ($P < 0.025$, $P < 0.05$, and $P < 0.005$, respectively). **C** and **D:** Light microscopic appearance (**C**) and hematoxylin and eosin (H&E)–stained sections (**D**) of *Rasa1*$^{R780Q/R780Q}$ and *Rasa1*$^{R780Q/fl}$ embryos and yolk sacs at E9.5. Features to note include reduced size and distended pericardial sac (**arrow**) and wrinkled appearance of the yolk sac of *Rasa1*$^{R780Q/R780Q}$ embryos. **E:** MEFs derived from E9.5 *Rasa1*$^{R780Q/R780Q}$ and *Rasa1*$^{fl/fl}$ embryos were analyzed for RASA1 protein abundance by using Western blot analysis. Blots were reprobed for glyceraldehyde-3-phosphate dehydrogenase (GAPDH) to show equivalent protein loading. Shown are RASA1 amounts in MEF derived from two different embryos of each genotype. E, embryo proper; YS, yolk sac.

the targeted *Rasa1* allele and deletion of the *NeoR* cassette (Figure 1B). Like heterozygous *Rasa1*-null mice,[17] heterozygous *Rasa1*^{R780Q} mice are healthy and do not show any BV abnormalities.

Heterozygous *Rasa1*^{R780Q} mice were crossed to mice with a conditional *Rasa1* allele in which exon 18 is flanked by *loxP* sites [floxed allele (*fl*)] (Figure 1B) to generate heterozygous *Rasa1*$^{R780Q/fl}$ mice.[25] The *Rasa1*$^{R780Q/fl}$ mice were then intercrossed, and genotypes of 3-week-old progeny were determined by PCR of tail genomic DNA using forward and reverse primers based in exon 18 and intron 18, respectively, that readily distinguish between the R780Q and floxed alleles (Figures 1B and 2A). In these experiments, no homozygous *Rasa1*$^{R780Q/R780Q}$ pups were identified using parental mice derived from either R780Q targeted ES cell line (Figure 2B). This is consistent with embryonic lethality of the *Rasa1*^{R780Q} mutation in homozygous form.

To determine the time of embryonic lethality, pregnancies were terminated at defined points after fertilization, embryos were harvested, and genotype was determined by PCR of yolk sacs (Figure 2B). At E9.5, homozygous *Rasa1*$^{R780Q/R780Q}$ embryos were identified in expected mendelian ratios. In contrast, at E11, a much less than expected number of *Rasa1*$^{R780Q/R780Q}$ embryos were identified (2 of 35 compared with an expected 9), and at E13.5, *Rasa1*$^{R780Q/R780Q}$ embryos were absent. These findings are consistent with midgestation lethality of *Rasa1*$^{R780Q/R780Q}$ mice, similar to that observed in *Rasa1*-null mice.[17,18]

At E9.5, *Rasa1*$^{R780Q/R780Q}$ embryos exhibited the same number of somites (20 to 25) as control *Rasa1*$^{R780Q/fl}$ and *Rasa1*$^{fl/fl}$ embryos. However, *R780Q/R780Q* embryos were considerably smaller than *R780Q/fl* and *fl/fl* embryos and appeared less developed (Figure 2, C and D). Other gross features of E9.5 *R780Q/R780Q* embryos included a

distended pericardial sac and wrinkled yolk sac compared with *Rasa1*$^{R780Q/fl}$ and *Rasa1*$^{fl/fl}$ embryos (Figure 2C) (data not shown). Both of these features were noted previously in *Rasa1*-null embryos at E9.5.[17] Furthermore, the same features were noted in the two identified *Rasa1*$^{R780Q/R780Q}$ E11 embryos (data not shown). To verify that midgestation embryonic lethality of *Rasa1*$^{R780Q/R780Q}$ embryos could be attributed specifically to the effect of the mutation on RASA1 catalytic activity and not any unforeseen influence on RASA1 protein stability, we prepared MEFs from E9.5 embryos and examined RASA1 protein abundance by using Western blot analysis. Amounts of RASA1 protein in *R780Q/R780Q* MEFs were unchanged compared with *fl/fl* MEFs (Figure 2E).

BV Abnormalities in Homozygous *Rasa1*^{R780Q} Mice

To study potential BV abnormalities in *Rasa1*$^{R780Q/R780Q}$ mice, we performed whole mount staining of E9.5 embryos using an anti-CD31 antibody to detect ECs (Figure 3A). In yolk sacs of *Rasa1*$^{fl/fl}$ and *Rasa1*$^{R780Q/fl}$ mice, organized BV networks that were continuous with the vasculature of the embryo proper were readily identified. In contrast, no such organized vascular networks were observed in the yolk sacs of *Rasa1*$^{R780Q/R780Q}$ mice. Instead, ECs were often identified in a honeycombed pattern, as described previously in homozygous *Rasa1*-null mice.[17] In the embryo proper of *Rasa1*$^{fl/fl}$ and *Rasa1*$^{R780Q/fl}$ mice, a normal dorsal aorta and intersegmental arteries that projected between somites were apparent. In contrast, the BV network of *R780Q/R780Q* embryos was abnormal (Figure 3A). In particular, the dorsal aorta showed a highly irregular shape. Furthermore, intersegmental arteries were frequently irregular in shape. To confirm these findings, serial sections of embryos were stained with CD31 antibodies to identify the dorsal aorta (Figure 3B). In control mice, the dorsal aorta was identified as a continuous structure that extended from the heart to the posterior of the embryo. In contrast, in *R780Q/R780Q* embryos, the dorsal aorta was severely disrupted. Similar abnormalities in BV architecture were

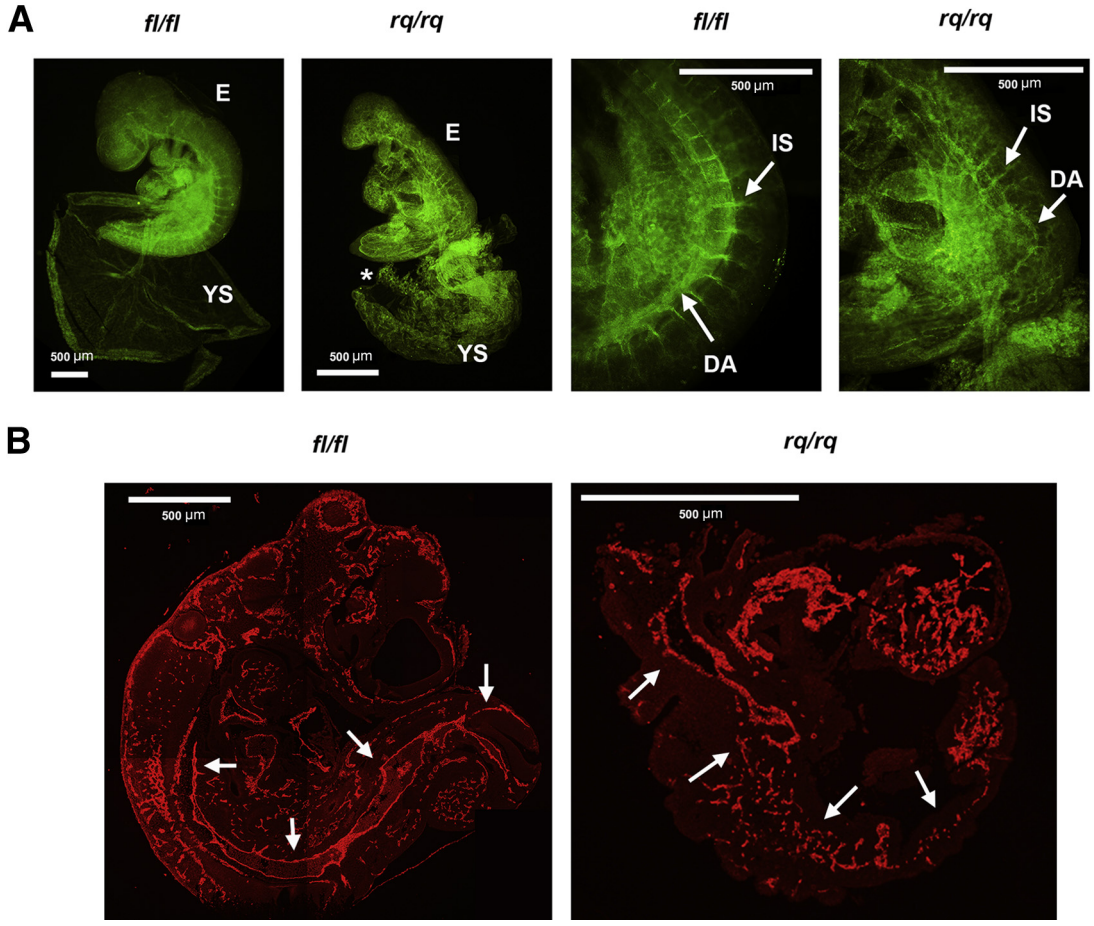

Figure 3 Cardiovascular abnormalities in homozygous *Rasa1*^{R780Q} mice. **A** and **B:** Whole mount (**A**) and sections (**B**) of E9.5 *Rasa1*$^{R780Q/R780Q}$ and *Rasa1*$^{fl/fl}$ embryos were stained with an anti-CD31 antibody to reveal blood vasculature. **A:** Note the organized BV network in the *Rasa1*$^{fl/fl}$ yolk sac (YS) and honeycombed appearance of blood vasculature in the *Rasa1*$^{R780Q/R780Q}$ yolk sac (**asterisk**). Note also irregular blood vasculature in the *Rasa1*$^{R780Q/R780Q}$ embryo proper (E). **B:** Note the disorganized dorsal aorta in the *Rasa1*$^{R780Q/R780Q}$ embryo compared with the *Rasa1*$^{fl/fl}$ embryo (**arrows**). DA, dorsal aorta; IS, intersegmental artery.

noted previously in E9.5 homozygous *Rasa1*-null embryos.[17]

Constitutive Activation of the Ras Signaling Pathway in ECs of Homozygous *Rasa1*^{R780Q} Mice

In its activated state, Ras triggers several different signaling cascades, including the MAPK pathway.[12,26] To confirm that MAPK was abnormally activated in BV of homozygous *Rasa1*^{R780Q} mice, sections from E9.5 embryos were stained with an antibody specific for phosphorylated activated forms of the ERK MAPK together with an anti-CD31 antibody (Figure 4). In control *Rasa1*$^{fl/fl}$ and *Rasa1*$^{fl/R780Q}$ embryos, most ECs were not stained with the anti-phosphorylated ERK (pERK) antibody. In contrast, in *Rasa1*$^{R780Q/R780Q}$ embryos, most ECs were pERK positive. Thus, MAPKs are constitutively activated in ECs of *Rasa1*$^{R780Q/R780Q}$ embryos.

Discussion

Most *RASA1* mutations in CM-AVM result in premature stop codons that are predicted to cause a loss of *RASA1* mRNA transcripts and RASA1 protein.[2,3] Potentially, therefore, BV abnormalities in these patients could develop as a consequence of loss of an ability of RASA1 to inhibit Ras activation or loss of Ras-independent functions of RASA1. Several Ras-independent functions of RASA1 have been described.[11] One Ras-independent function is directed cellular migration that has been observed in fibroblasts and is mediated by RASA1 SH2 domain recognition of the p190 RhoGAP protein that regulates actin cytoskeleton dynamics.[27] It has been suggested previously that impaired directed cellular migration of ECs may underlie the pathological abnormalities in CM-AVM.[28,29] Of the few *RASA1* missense mutations that have been identified in CM-AVM, it is currently unknown how they would affect Ras-dependent or RAS-independent functions of RASA1 or RASA1 protein stability.

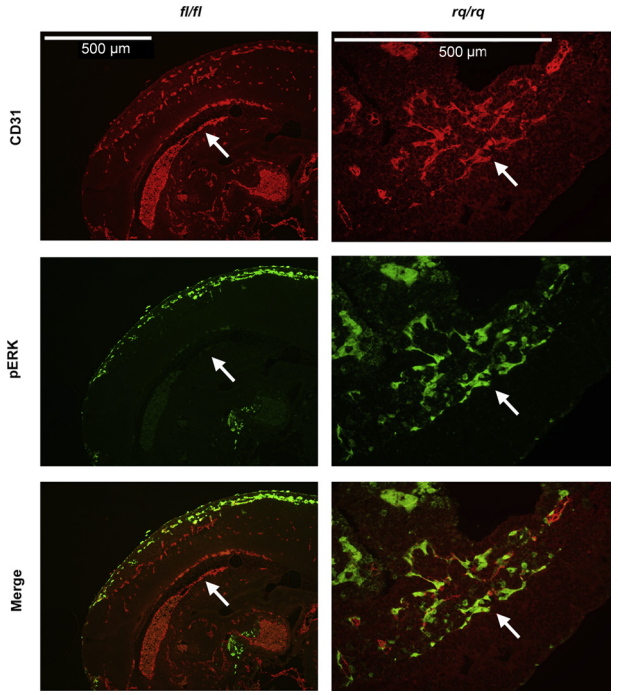

Figure 4 MAPK activation in homozygous *Rasa1*^{R780Q} embryos. Tissue sections of E9.5 *Rasa1*$^{R780Q/R780Q}$ and *Rasa1*$^{fl/fl}$ embryos were stained with anti-CD31 (red) and anti–phospho-ERK (green) antibodies. Shown are select regions of embryos that include part of the dorsal aorta (**arrows**). Note the absence of pERK staining in most ECs in *Rasa1*$^{fl/fl}$ embryos and the presence of pERK staining in most ECs in *Rasa1*$^{R780Q/R780Q}$ embryos.

To shed light on how loss of RASA1 might lead to BV abnormalities in CM-AVM, we generated *Rasa1*^{R780Q} knockin mice. Arginine 780 constitutes the arginine finger of the RASA1 GAP domain that is 100% conserved and is essential for RASA1 to promote Ras hydrolysis of bound GTP.[11,16] On RASA1 interaction with Ras-GTP, the RASA1 arginine finger is inserted into the Ras active site, which permits glutamine 61 of Ras to participate in catalysis.[16] As shown previously, mutation of the arginine finger to a glutamine abrogates an ability of RASA1 to promote Ras-GTP hydrolysis but does not affect overall protein structure.[19] Homozygous *Rasa1*$^{R780Q/R780Q}$ mice showed abnormal BV development in both the yolk sac and embryo proper and died in midgestation at approximately E10 to E11. In these respects, the phenotype of *Rasa1*$^{R780Q/R780Q}$ mice is identical to that of *Rasa1*-null mice. These findings, therefore, support the contention that BV abnormalities in CM-AVM result from loss of an ability of RASA1 to regulate Ras in ECs and not from loss of a Ras-independent function of this molecule.

Consistent with the effect of the *Rasa1*^{R780Q} mutation on RASA1 catalytic activity, MAPK activation was increased in ECs of *Rasa1*$^{R780Q/R780Q}$ embryos at E9.5 (Figure 4). Thus, most ECs in mutant embryos stained strongly with phospho-MAPK antibodies. In contrast, few ECs in control E9.5 embryos were phospho-MAPK positive, including in the dorsal aorta, as reported previously.[30] Notably, increased pERK staining in *Rasa1*$^{R780Q/R780Q}$ embryos was largely confined to ECs, despite the broad expression of RASA1. This indicates that in non-EC types in these embryos, other Ras-GAPs compensate for the loss of RASA1 catalytic activity in the regulation of Ras-MAPK signaling. In turn, this might explain why phenotypes in mice and humans with *Rasa1*/*RASA1* mutations are relatively restricted to the BV compartment.

Which growth factor receptors use RASA1 to inhibit Ras activation during BV development is uncertain. One recent study in zebrafish has indicated that RASA1 functions downstream of the Ephrin B4 receptor to control BV development, although this has yet to be confirmed in mammals.[31] In addition, which downstream effectors of Ras drive BV abnormalities in RASA1-deficient mice and humans is currently unknown. As well as MAPK, PI3K and other downstream effectors of Ras could contribute to the development of lesions. In this regard, PI3K lies upstream of the

mechanistic target of rapamycin that has been shown to be hyperactivated in CM-AVM BV.[31] Potentially, therefore, inhibitors of any of MAPK, PI3K, or mechanistic target of rapamycin alone or in combination may prove effective in the treatment of BV abnormalities in this condition.

References

1. Eerola I, Boon LM, Mulliken JB, Burrows PE, Dompmartin A, Watanabe S, Vanwijck R, Vikkula M: Capillary malformation-arteriovenous malformation, a new clinical and genetic disorder caused by RASA1 mutations. Am J Hum Genet 2003, 73:1240−1249
2. Revencu N, Boon LM, Mulliken JB, Enjolras O, Cordisco MR, Burrows PE, Clapuyt P, Hammer F, Dubois J, Baselga E, Brancati F, Carder R, Quintal JM, Dallapiccola B, Fischer G, Frieden IJ, Garzon M, Harper J, Johnson-Patel J, Labreze C, Martorell L, Paltiel HJ, Pohl A, Prendiville J, Quere I, Siegel DH, Valente EM, Van Hagen A, Van Hest L, Vaux KK, Vicente A, Weibel L, Chitayat D, Vikkula M: Parkes Weber syndrome, vein of Galen aneurysmal malformation, and other fast-flow vascular anomalies are caused by RASA1 mutations. Hum Mutat 2008, 29:959−965
3. Revencu N, Boon LM, Mendola A, Cordisco MR, Dubois J, Clapuyt P, et al: RASA1 mutations and associated phenotypes in 68 families with capillary malformation-arteriovenous malformation. Hum Mutat 2013, 34:1632−1641
4. Bayrak-Toydemir P, Stevenson D: RASA1-Related Disorders. Edited by RA Pagon, MP Adam, HH Ardinger, et al. In GeneReviews [Internet]. Copyright University of Washington, Seattle. 2011. Available at http://www.ncbi.nlm.nih.gov/books/NBK52764, last revised December 19, 2013
5. de Wijn RS, Oduber CE, Breugem CC, Alders M, Hennekam RC, van der Horst CM: Phenotypic variability in a family with capillary malformations caused by a mutation in the RASA1 gene. Eur J Med Genet 2012, 55:191−195
6. Hershkovitz D, Bercovich D, Sprecher E, Lapidot M: RASA1 mutations may cause hereditary capillary malformations without arteriovenous malformations. Br J Dermatol 2008, 158:1035−1040
7. Hershkovitz D, Bergman R, Sprecher E: A novel mutation in RASA1 causes capillary malformation and limb enlargement. Arch Dermatol Res 2008, 300:385−388
8. Thiex R, Mulliken JB, Revencu N, Boon LM, Burrows PE, Cordisco M, Dwight Y, Smith ER, Vikkula M, Orbach DB: A novel association between RASA1 mutations and spinal arteriovenous anomalies. AJNR Am J Neuroradiol 2010, 31:775−779
9. Wooderchak-Donahue W, Stevenson DA, McDonald J, Grimmer JF, Gedge F, Bayrak-Toydemir P: RASA1 analysis: clinical and molecular findings in a series of consecutive cases. Eur J Med Genet 2011, 55:91−95
10. Conti E, Izaurralde E: Nonsense-mediated mRNA decay: molecular insights and mechanistic variations across species. Curr Opin Cell Biol 2005, 17:316−325
11. King PD, Lubeck BA, Lapinski PE: Nonredundant functions for Ras GTPase-activating proteins in tissue homeostasis. Sci Signal 2013, 6:re1
12. Buday L, Downward J: Many faces of Ras activation. Biochim Biophys Acta 2008, 1786:178−187
13. Castellano E, Downward J: Role of RAS in the regulation of PI 3-kinase. Curr Top Microbiol Immunol 2010, 346:143−169
14. Castellano E, Downward J: RAS interaction with PI3K: more than just another effector pathway. Genes Cancer 2011, 2:261−274
15. Rubinfeld H, Seger R: The ERK cascade: a prototype of MAPK signaling. Mol Biotechnol 2005, 31:151−174
16. Scheffzek K, Ahmadian MR, Kabsch W, Wiesmuller L, Lautwein A, Schmitz F, Wittinghofer A: The Ras-RasGAP complex: structural basis for GTPase activation and its loss in oncogenic Ras mutants. Science 1997, 277:333−338
17. Henkemeyer M, Rossi DJ, Holmyard DP, Puri MC, Mbamalu G, Harpal K, Shih TS, Jacks T, Pawson T: Vascular system defects and neuronal apoptosis in mice lacking ras GTPase-activating protein. Nature 1995, 377:695−701
18. Lapinski PE, Kwon S, Lubeck BA, Wilkinson JE, Srinivasan RS, Sevick-Muraca E, King PD: RASA1 maintains the lymphatic vasculature in a quiescent functional state in mice. J Clin Invest 2012, 122:733−747
19. Miao W, Eichelberger L, Baker L, Marshall MS: p120 Ras GTPase-activating protein interacts with Ras-GTP through specific conserved residues. J Biol Chem 1996, 271:15322−15329
20. Charles MA, Saunders TL, Wood WM, Owens K, Parlow AF, Camper SA, Ridgway EC, Gordon DF: Pituitary-specific Gata2 knockout: effects on gonadotrope and thyrotrope function. Mol Endocrinol 2006, 20:1366−1377
21. Soliman GA, Ishida-Takahashi R, Gong Y, Jones JC, Leshan RL, Saunders TL, Fingar DC, Myers MG Jr: A simple qPCR-based method to detect correct insertion of homologous targeting vectors in murine ES cells. Transgenic Res 2007, 16:665−670
22. Oliver JA, Stolberg VR, Chensue SW, King PD: IL-4 acts as a potent stimulator of IFN-gamma expression in CD8+ T cells through STAT6-dependent and independent induction of Eomesodermin and T-bet. Cytokine 2012, 57:191−199
23. Schmittgen TD, Livak KJ: Analyzing real-time PCR data by the comparative C(T) method. Nat Protoc 2008, 3:1101−1108
24. Rodriguez CI, Buchholz F, Galloway J, Sequerra R, Kasper J, Ayala R, Stewart AF, Dymecki SM: High-efficiency deleter mice show that FLPe is an alternative to Cre-loxP. Nat Genet 2000, 25:139−140
25. Lapinski PE, Bauler TJ, Brown EJ, Hughes ED, Saunders TL, King PD: Generation of mice with a conditional allele of the p120 Ras GTPase-activating protein. Genesis 2007, 45:762−767
26. Chang L, Karin M: Mammalian MAP kinase signalling cascades. Nature 2001, 410:37−40
27. Kulkarni SV, Gish G, van der Geer P, Henkemeyer M, Pawson T: Role of p120 Ras-GAP in directed cell movement. J Cell Biol 2000, 149:457−470
28. Dejana E, Tournier-Lasserve E, Weinstein BM: The control of vascular integrity by endothelial cell junctions: molecular basis and pathological implications. Dev Cell 2009, 16:209−221
29. Uebelhoer M, Boon LM, Vikkula M: Vascular anomalies: from genetics toward models for therapeutic trials. Cold Spring Harb Perspect Med 2012, 2. pii:a009688
30. Lan Y, He W, Li Z, Wang Y, Wang J, Gao J, Wang W, Cheng T, Liu B, Yang X: Endothelial Smad4 restrains the transition to hematopoietic progenitors via suppression of ERK activation. Blood 2014, 123:2161−2171
31. Kawasaki J, Aegerter S, Fevurly RD, Mammoto A, Mammoto T, Sahin M, Mably JD, Fishman SJ, Chan J: RASA1 functions in EPHB4 signaling pathway to suppress endothelial mTORC1 activity. J Clin Invest 2014, 124:2774−2784